RESILIENT INFRASTRUCTURE
June 1–4, 2016
RESILIENT INFRASTRUCTURE LONDON 2016

NUMERICAL MODELING FOR STRUCTURAL BEHAVIOR OF BRIDGE DECK BARRIERS MADE OF FIBER REINFORCED CONCRETE

Saman Hedjazi
Ryerson University, Canada

Hamidreza Khederzadeh
Ryerson University, Canada

Khaled Sennah
Ryerson University, Canada

ABSTRACT

Nonlinear finite-element (NLFE) analysis was used to compare and optimize the load transfer and failure mode of bridge barriers subjected to static transverse loads. Concrete is a material that needs strengthening in tension in order to meet the structural requirements. Studies have shown that the addition of steel fibers in a concrete matrix improves all the mechanical properties of concrete, especially tensile strength, impact strength, and toughness. The resulting material possesses higher tensile strength, consolidated response and better ductility. Although fiber reinforcement is a method that has been in use over the last few decades, yet it is unfamiliar to some practices, and there is no common guideline for design using this method. It is now well established that one of the important properties of fiber reinforced concrete (FRC) is its superior resistance to cracking and crack propagation and also the fibers are able to hold the matrix together even after extensive cracking. In the present study, numerical finite-element analysis has been performed on selected bridge barriers with steel reinforcement, to compare the difference between barriers with normal and fiber reinforced concrete. The FE modeling was performed under static load testing with displacement control. The ultimate load carrying capacities for each barrier type was compared. The behaviors of FRC barriers with different amount of fibers were accurately simulated with NLFE models. Modifications were then made to FRC barriers to reduce the barrier wall thickness as well as the reinforcement arrangement. The present study shows reserved capacity of FRC barriers compared to their counterparts with normal concrete and steel reinforcement.

Keywords: Bridges; Bridge Barrier; Size effect; Fiber-reinforced concrete; Nonlinear finite element calculations.

1. INTRODUCTION

Fiber reinforcement is a method that has been in use over the last few decades, yet it is unfamiliar to some practices, and there is no common guideline for design using this method. It is now well established that one of the important properties of fiber reinforced concrete (FRC) is its superior resistance to cracking and crack propagation and also the fibers are able to hold the matrix together even after extensive cracking. Early technological development of steel fiber reinforced concrete (SFRC) was hampered by lack of information and authenticated measures until the early 1960's. Since that, researchers have done extensive researches on SFRC, driven by the promising performance enhancements in terms of strength, durability and toughness. Studies have shown increasing evidence that the brittle behavior of concrete can be overcome by the addition of short steel fibers of small diameters in the concrete mix [1, 2]. ACI Committee 544[3] reported that the addition of steel fibers in a concrete matrix improves all mechanical properties of concrete, especially tensile strength, impact strength, and toughness. Identifying the correlation between the tensile strength as the dependent variable and each of the aspect ratio and the volumetric ratio as independent variables is an important aspect of successful design. Concrete fiber composites have been found more economical for use in Airport and Highway Pavements, Bridge Decks, Erosion resistance structures, slope stabilization, Refractory concrete, Earthquake resistance structures and Explosive resistance structures [4]. In the

design of concrete structures, the two essentially considered material properties are compressive and tensile strengths. Compressive strength is a major parameter in the case of structural applications, whereas flexural strength is an essential parameter in pavement applications. In certain applications, toughness is a vital parameter [5]. The observations given by published literature indicate that the selection of SFRC volumetric fraction can be chosen within the range of 1 to 2.5% by concrete absolute volume [6]. Few studies have been carried out towards investigating the relationship between the split tensile strength and the compressive strength of SFRC. The available relationships are either based on limited number of specimens or narrow range of fiber content or fiber aspect ratio. Ashour et al [7,8] suggested the following equation for high strength concrete specimens of a single aspect ratio, *l/d* of 75

[1] $f\,sp = 4.95 - 2.13\,v\,f$

Where $v\,f$ is the volumetric fiber content. Studies carried out by Yazici et al. [9], Holschemacher et al.[10] and others concluded that in case of SFRC, volumetric fraction as well as the aspect ratio (l/d) are two major factors in terms of performance enhancement.

More parameters were presented within the expression addressed by Ashour et al. [11], as follows:

[2] $f\,sp = (0.6 + 0.4\,(v\,f \times l/d\,)) \times \sqrt{f\,c}$

In the present study constitutive model for FRC in compression is assumed based on the equation below:

[3] $$\frac{\sigma_c}{f_c} = \frac{\beta\left(\frac{\varepsilon_c}{\varepsilon_{c,0}}\right)}{\beta - 1 + \left(\frac{\varepsilon_c}{\varepsilon_{c,0}}\right)^{\beta}}$$

[4] $$\beta = \left(0.0536 - 0.5754 V_f\right) f_c$$

[5] $$\varepsilon_{c,0} = \left(0.00048 + 0.01886\, V_f\right) \ln f_c$$

Where the details and parameters are derived by Carreira et al. and Nataraja [12,13], and the aspect ratio, *l/d and* the volumetric fiber content, $v\,f$, are considered in the equations.

2. FINITE ELEMENT MODELING OF CONCRETE BARRIERS

Although the experimental programs are compulsory for a research to progress, the problems can be simplified with advances in modern computers using finite-element software. ABAQUS (Hibbitt et al. 2011) is regarded as sophisticated and general purpose software that can be utilized to model the behavior of structural members under externally applied load.

In this paper, finite-element models, describing the non-linear behavior of steel and fiber-reinforced concrete bridge barriers under static load testing were developed. The non-linear finite element package “ABAQUS” was utilized for this purpose. Numerical simulations on the structural response of statically loaded bridge barriers and the associated failure modes have been performed herein by the ABAQUS/ Explicit, which is suitable for static test events and strong discontinuous geometrical or material response (Hibbitt et al. 2011). The concrete barrier was reinforced with conventional steel reinforcement in the deck slab and the barrier wall. As such, the concrete damaged plasticity (CDP) model and elastic-perfectly plastic with isotropic hardening material models have been used to define the static behavior of concrete and reinforcing steel, respectively. Concrete damaged plasticity model in ABAQUS/Explicit is capable of modeling the behavior of plain and reinforced concrete structures or other quasi-brittle materials subjected to static, cyclic or dynamic loading. The tensile behavior of concrete after failure is modeled in ABAQUS with tension stiffening. The tension stiffening allows defining the strain-softening branch of concrete after failure due to bond interaction between concrete and the reinforcement. Concrete behave differently in

tension and compression. It is very strong in compression compared with its tension behavior. The tensile strength of concrete is relatively low (about 8% to 15% of the compressive strength). Figure 1, illustrates typical stress-strain curve of concrete behavior in tension and in compression. In tension, concrete is loaded until it reaches the tensile cracking strength, $f't$, after which the stress-strain curve follows by some tension stiffening branch if reinforcement presents. In compression, concrete is loaded until it reaches the peak compressive strength, $f'c$, followed by crushing of concrete with increase in compressive straining. Two types of material properties were defined to represent non-linear properties of concrete material namely as elastic and plastic properties. Table 1 presents the concrete compressive strength considered herein for FE modeling of the proposed barriers. Steel reinforcing bars are modeled as a linear-elastic material up to the point of yielding. After yielding, a yield plateau occurs followed by either a linear or non-linear strain hardening phase until rupture.

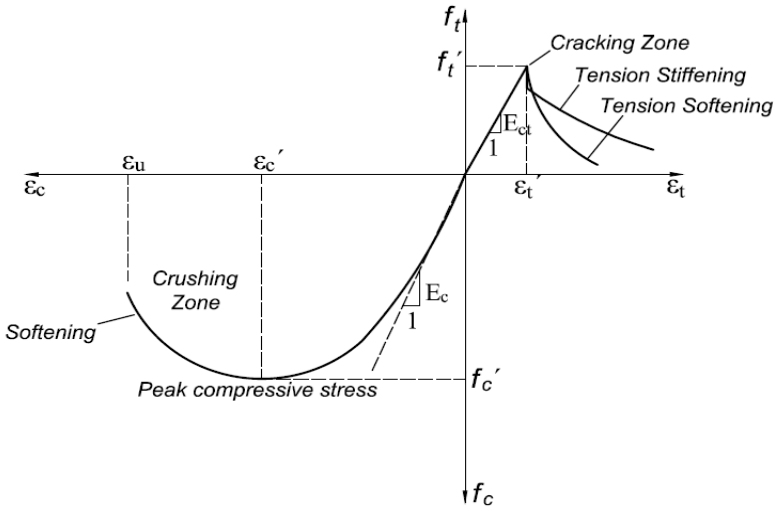

Figure 1: Typical stress-strain curve of concrete in tension and compression (Adopted from Khederzadeh et al.)

Table 1. Concrete compressive strengths assumed for barriers

Barrier model	Concretecompressive strength (MPa)	Elastic modulus (MPa)
Short barrier	25.4	22,680
Long barrier	30.9	25,015

In FE modeling, evolution of the yield criterion is based on the uniaxial elastic behavior of material models; thus, the definition of material parameters and uniaxial material behavior is more important. CSA A23.3 specifies approximate elastic modulus of normal density concrete with a density of about 2300 kg/m3 as follow;

[6] $Ect = 4500\sqrt{f'c}$ (MPa) (in tension)

[7] $Ec = 2\ f'c/\varepsilon'c \cong 4500\sqrt{f'c}$ (MPa) (in compression)

Where, Ect is the initial tangent stiffness of concrete, and $f'c$ is concrete compressive strength estimated from experimental concrete test cylinders. Values of the elastic modulus of numerically tested barriers are calculated using equation 6 and provided in Table 1. Solid 3D elements with 8 nodes linear brick and reduced integration with hourglass control (C3D8R), were used to mesh the concrete barrier wall. Also, the 3D stress-linear displacement truss elements with 2 nodes (T3D2) were used to model the reinforcing bars.

3. DETAILS OF CONCRETE BARRIERS

The FE modeling was carried out on the selected 1-m short barrier as well as the long barrier models. The short length barrier represents the case for one-way action behavior of barriers under static load testing so that only horizontal flexural cracks are expected in the wall portion and deck-wall junction. However, the long barrier represents structural behavior of tested barriers by two-way actions, in which the failure of the wall expected to include horizontal flexural cracks as well as the diagonal shear cracks. In all barrier models, steel reinforcement was used as reinforcing bars in the deck slab and the wall portion. In the deck portion, M25 steel bars were used at tension face, while M15 steel bars used at compression face of the deck slab. However, in the barrier wall, M15 bars were used to reinforce the barrier wall everywhere, except M12 bars were used as vertical bars at back face of the wall. Figure 2 shows view of the PL-3 traffic barrier with reinforcement arrangement in the wall.

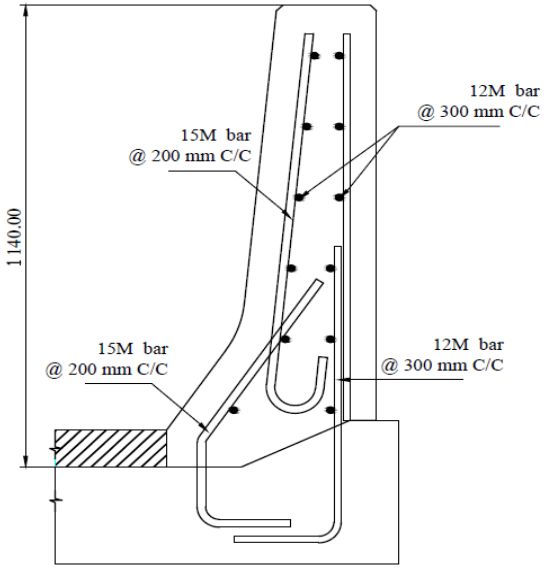

Figure 2: Selected barrier models for numerical analysis

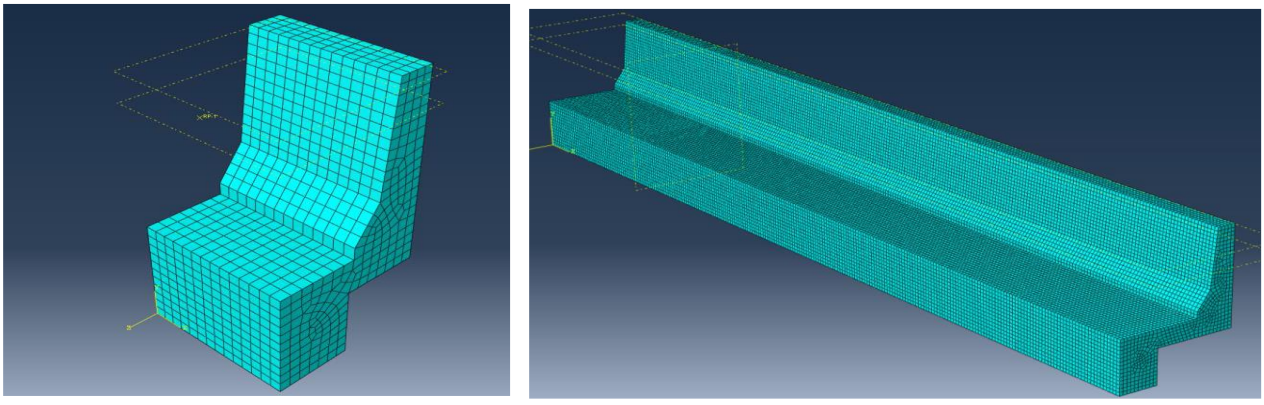

(a) Short barrier (b) Long barrier

Figure 3: Barrier models with finite-element meshing

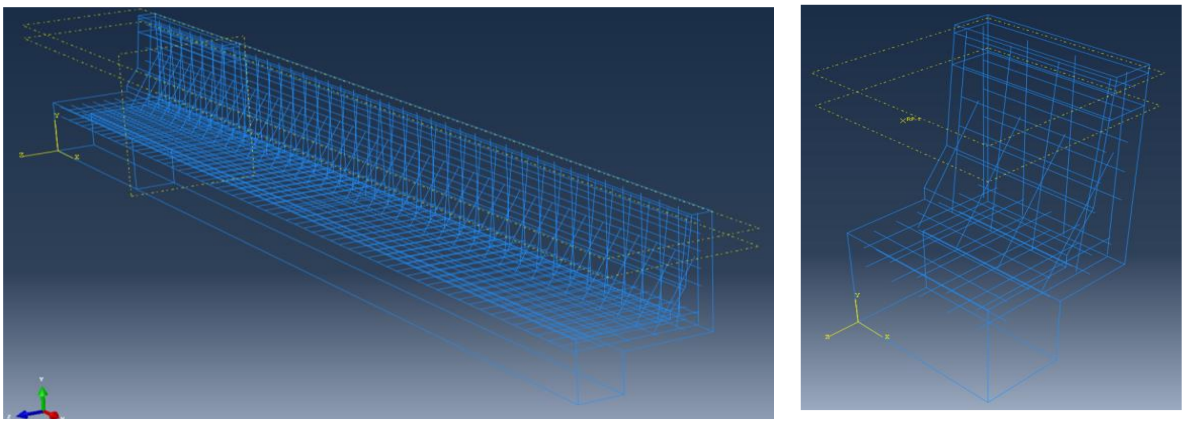

Figure 4: Rebar arrangements in the deck and the barrier walls

4. RESULTS AND DISCUSSIONS

In this section, the ability of ABAQUS/Explicit to model the behavior of traffic barrier walls under static load testing has been investigated. The ABAQUS/Explicit version 6.13 was used to model the barriers. 3D FE models were generated based on proposed geometry and load conditions of the PL-3 barriers approved by Ministry of Transportation of Ontario. Figure 3 and 4, show geometry of the barrier models and arrangement of transverse and longitudinal reinforcement in the wall and deck slab portion.

The numerical simulation is meaningful when the results are similar to those of the actual model. To validate FE model accuracy, geometry, shape and material properties should be imported from actual model to the FE model. The output results in terms of load-displacement, strains and stresses should yield relatively similar values. Therefore, numerical models were conducted using the same material properties for normal concrete and fiber-reinforced concrete as in the literatures. Such FE modeling are considered as the preliminary design of the fiber-reinforced barrier to obtain ultimate load carrying capacities compared with barriers with normal concrete. The numerical analysis are revised with results obtained from actual testing of the proposed barrier walls and can be reached elsewhere (Khederzadeh et al. [15]), where for each model, the load-displacement curve, the barrier wall lateral displacement and crack patterns were obtained from ABAQUS. The FE modeling was carried out on a barrier to examine the accuracy of the FE modeling (Figure 5). When the accuracy of the model was confirmed with the small scale barriers, the material property definition was taken similarly to model the large scale barrier at interior location. The following subsections discuss the FE results of each barrier model in more detail. Figure 6 shows the configuration of a PL3 barrier for another experimental study conducted on an actual scale long barrier (Khederzadeh et al. [15]), and is going to be compared with the FRC barriers in the present study.

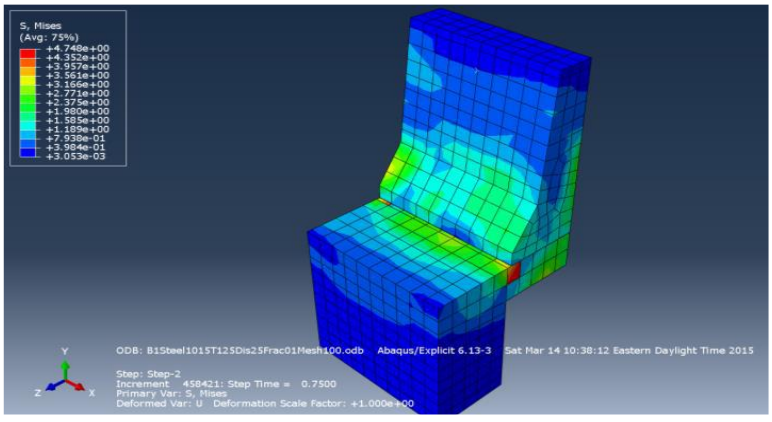

Figure 5: Overall shape of barrier failure by Von-Mises criterion

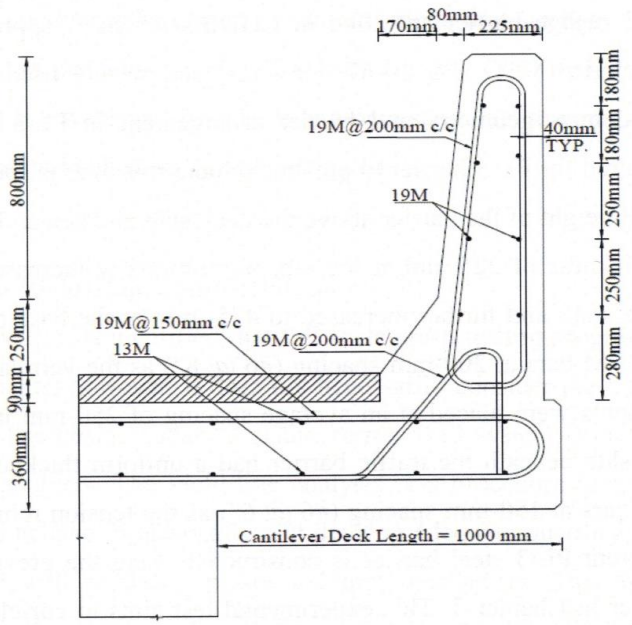

Figure 6: Long Barrier - PL3 configuration used in experimental study

After evaluation of the reliability of the FE model and calibrate some unknown parameters with uncertainty, and comparison between the FE models results with the experimental load-displacement responses as well as the obtained crack patterns from testing of the barriers, and prior to conducting non-linear analysis of barrier with fiber-reinforced concrete, the barrier (Figure 2) with normal reinforced concrete was modeled. In non-linear analysis, it was assumed that the barrier is subjected to a lateral displacement of 25 mm which was applied 990 mm above the deck slab. The ABAQUS program was to apply the 25 mm displacement into 20 increments. From the FE modeling of the normal reinforced concrete barriers, the barrier was failed at a load of 107 kN.

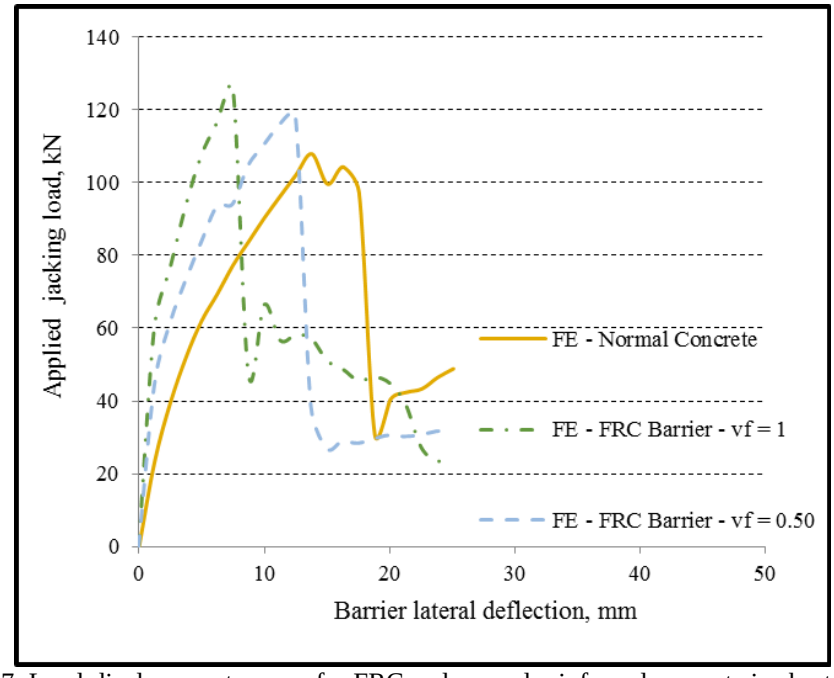

Figure 7: Load-displacement curves for FRC and normal reinforced concrete in short barriers

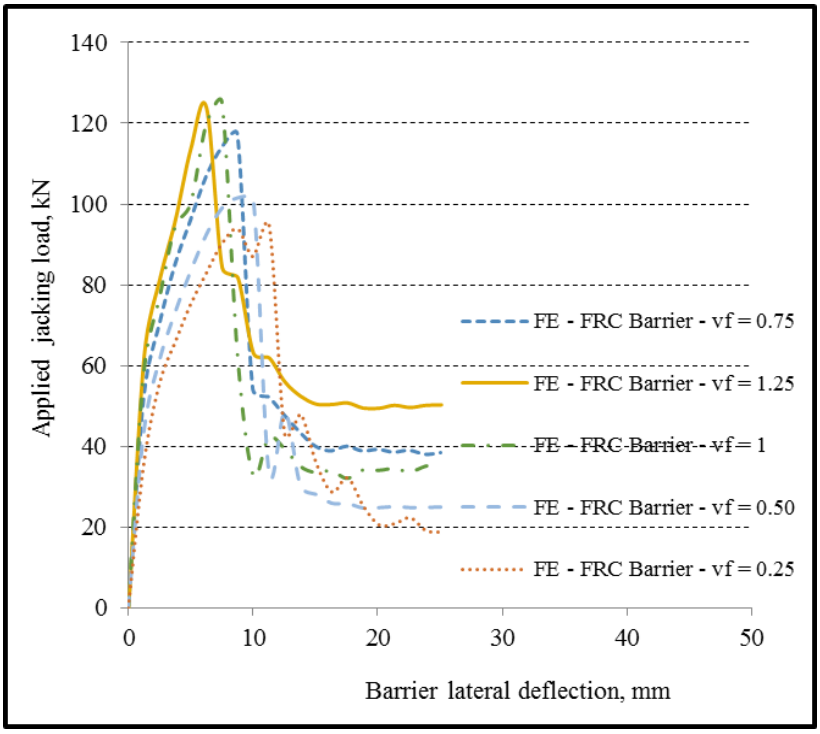

Figure 8: Load-displacement curves for FRC short barriers

Once the barrier with steel reinforced was modeled and calibrated, material properties for fiber-reinforced concrete with 0.25% , 0.5 %, 0.75%, 1% and 1.25% fiber volume fraction was obtained from current literature and imported into ABAQUS. Figure 7, also compared graph of load-displacement curve of FRC barrier with that of normal concrete barrier. It should be noted that in both barriers with normal and fiber-reinforced concretes, the barriers were modeled with similar arrangement of steel bars in the wall and the deck portion. From the FE model, the FRC barrier was failed at a load of 119 kN and 126 kN for 0.5 %, and 1% fiber volume fraction respectively. Figure 8, compared graph of load-displacement curve of FRC barrier with 0.25% , 0.5 %, 0.75%, 1% and 1.25% fiber volume fraction. It shows that in fiber-reinforced concretes barriers, the ultimate load carrying capacity of barriers are increased with the increase in the amount of fiber volumes, and the analysis demonstrates that the optimum values are reached with the 1% of fiber volume fraction.

From the analysis, it was noticed that the ultimate load carrying capacity of FRC barrier improved 18% in the application of FRC with 1% fiber volume fraction compared to normal concrete, so prior to failure of the barrier for the same displacement, the FRC barrier reserved relatively higher load when compared to normal concrete barrier. In normal concrete barrier, the first crack appeared at displacement of 1.25 mm and load of 42 kN, however, in FRC barrier with the same displacement, the load was 56 kN which corresponds to an increase of 33.1% in the applied load.

The post-failure behavior and residual stress in FRC barrier improved comparably with normal concrete barrier. From this observation, it was decided to reduce the geometry of the FRC barrier. Therefore, in the FE modeling of long barriers a reduction of 50 mm in the geometry of the barrier shown in Figure 2 was considered but the bar arrangement was kept the same (namely called it 175mm barrier in figures versus 225 mm barrier illustrated in figure2), also a long barrier with the exact geometry of figure 2 (225 mm barrier) is modeled for verification.

Similar to the FE modeling of the short length barriers, the long barriers are also being modeled and loaded at interior location with normal and fiber-reinforced concretes and the results were compared. Similar material property definitions to experimental study were considered in the long barrier models. The barriers at interior location were modeled based on the principle of symmetry. Therefore, the results shown herein are on the half-length of the barrier. In accordance with CHBDC, the transverse displacement was applied over an area of 2400 x 200 mm2 with the centroid of the displacement at 990 mm above the deck slab. Similar barrier geometry and bar

arrangement as the short barrier were considered in numerical study. As displacement of 40 mm was applied on the top of the wall in 20 increments and load-displacement curves were captured from ABAQUS for each of normal and FRC barrier. Figure 9 compared the load-displacement of modeled barrier with FRC for the long barriers with rebar configuration of figure 2 and length of 12 meters but the thickness of the barriers are reduce to 175mm instead of 225 mm. From the graphs, it can be observed that the increase in the amount of fibers increases the load bearing capacity in long barriers also. It is obvious that the increase in fiber volume fraction from 0.75% to 1 % shows a 36 % growth in ultimate load carrying capacity from 535 kN to 730 kN respectively.

The cracking stress concentrations in the wall and deck portion of the barriers were investigated. ABAQUS shows smeared crack models at stress or strain cracking rate. Figure 11 (a) depicts overall failure of the barrier by von-mises theory. It can be observed that the barrier wall experience flexural cracks at the deck-wall junction as well as the tapered portion of the wall, followed by diagonal shear cracks that are extended to the top of the wall causing punching shear in the wall portion at the top.

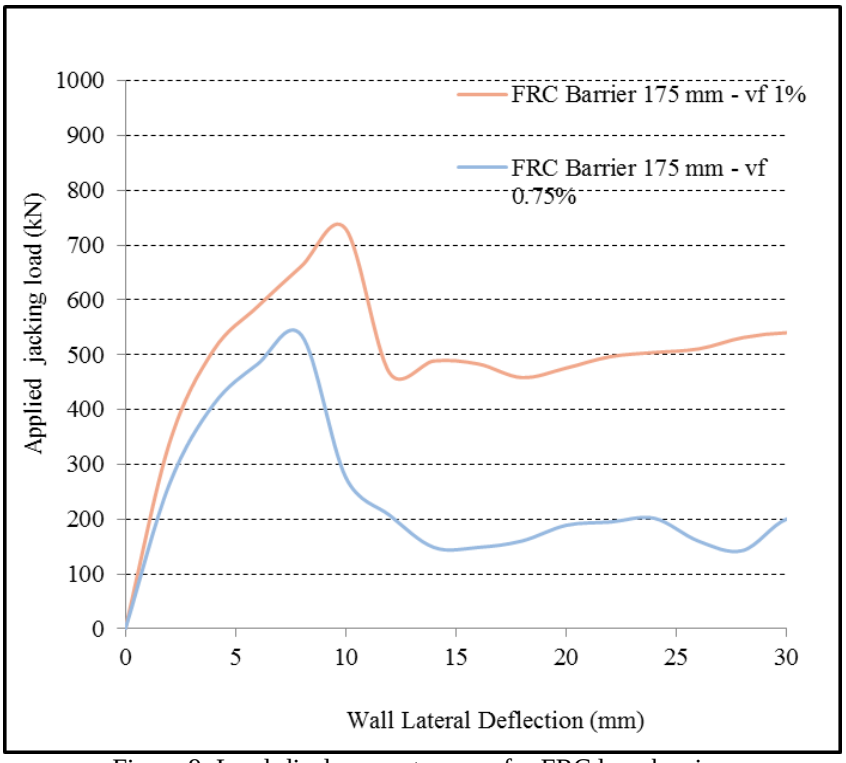

Figure 9: Load-displacement curves for FRC long barriers

Figure 10 compares the graphs of load-displacement curves for the two numerically modeled FRC barriers. One barrier with the same geometry shown in figure 2 (225 mm thickness) and the other with the reduced wall thickness to 175mm, both with the same rebar arrangement as Figure 2. Figure 10 , also, illustrates the experimental result for the barrier whit the configuration in Figure 6 and normal concrete. It can be observed that the implementation of FRC can compensate the difference in rebar sizes between the two type of barriers shown in Figure 2 and Figure 6, and as a result lead to more economic design. In all barrier models, the ultimate load in FRC barriers were increased, and at the same time the ductility of the FRC barriers were significantly enhanced. Figures 11(b) shows views overall barrier failure by von-mises failure criterion, it can be observed that the barrier wall experience shear and punching shear cracks at the applied load location at the vertical portion of the wall, diagonal shear cracks reach to the top of the wall causing punching shear in the wall portion at the top.

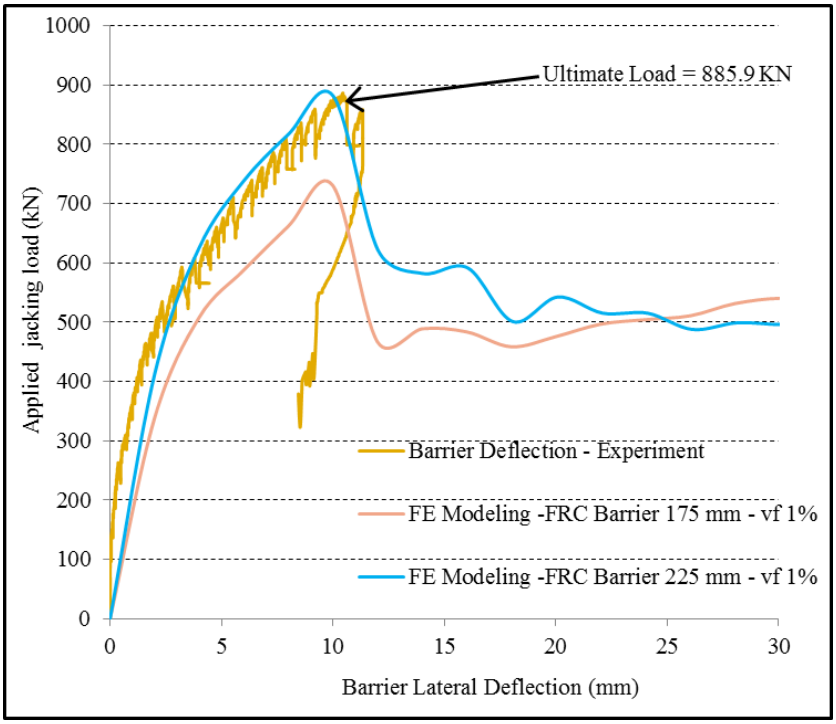

Figure 10: Load-displacement curves for FRC long barriers compared to experimental results

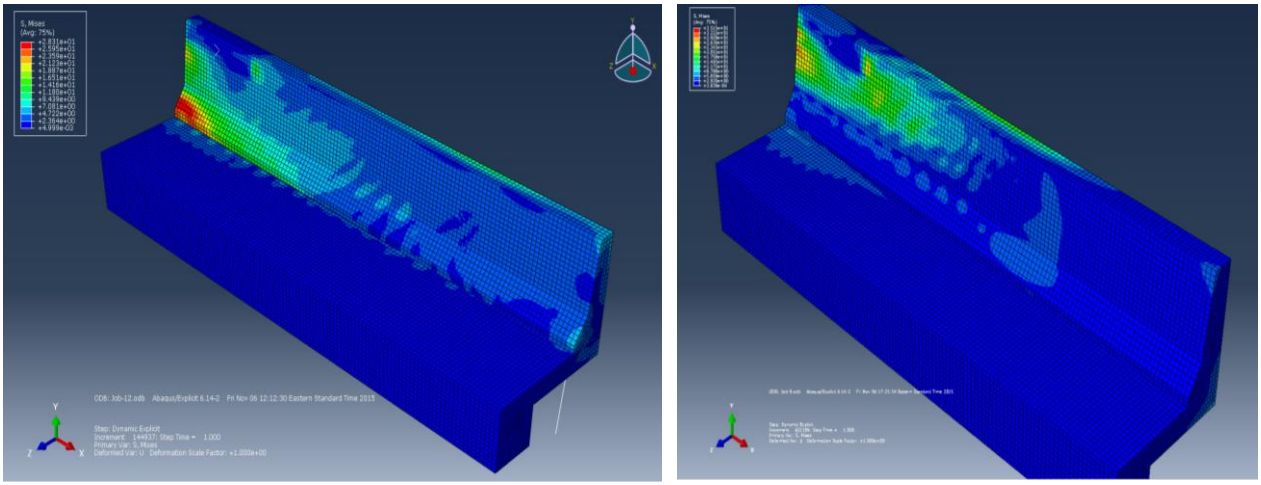

(a) Long barrier with minimum thickness of 175mm (b) Long barrier with minimum thickness of 225 mm

Figure 11: Overall failure of the barrier at interior location by Von-Mises criterion

5. CONCLUSION

The NLFE models created for this study accurately reproduced the experimental results in terms of stiffness, crack damage, and failure mode. The results demonstrate that all FRC barriers configurations exceed the static design criteria specified in the CSA bridge design codes and meet the recommended failure hierarchy for bridge barrier design. Finite-element modeling of fiber-reinforced concrete barriers were investigated under static load testing and compared with normal reinforced concrete and experimental results. The NLFE model accurately reproduced the experimental results for the pre- and post-cracking tensile strength properties, so FE modeling can be utilized for the preliminary design of the barrier to obtain ultimate load carrying capacity and expected failures of the barrier. FE modeling carried on the FRC barriers improve the ultimate load carrying capacity of the barriers, and comparably

increased the ductility of the barrier both at pre-peak and post-peak behavior. This feature of the FRC's can enhance the resistance to the impact loading of the barrier and increase the energy absorbance. The first crack appeared relatively at higher load in FRC barriers when compared to the normal-reinforced concrete barriers. This indicates an increase in the tensile strength of the FRC barriers compared to normal concrete barriers. Due to such increase in the barrier ductility and tensile strength of the concrete, it presumed that barrier enhancement can be made for FRC barriers, for example; the wall thickness can be reduced from top or bottom or along the height, wall reinforcement can be reduced at front and back face of the wall, also it might be advisable to remove the back face reinforcement.

ACKNOWLEDGMENTS

This study was sponsored by Ontario Ministry of Transportation's (MTO) Highway Infrastructure Innovation Funding Program. Such support is greatly appreciated. Opinions expressed in this paper are those of the authors and do not necessarily reflect the views and policies of the Ministry.

REFERENCES

[1] D.A. Fanella and A.E. Naaman, 1985. "Stress-strain properties of fiber reinforced mortar in compression", ACI Journal, 82(4), pp.475-583.

[2] L.S. Hsu and C.T.T. Hsu, 1994. "Stress-strain behavior of steel fiber reinforced high strength concrete under compression", ACI Materials Journal, 91(4), pp.448- 457.

[3] ACI Committee 544, 1996. "State of the art report on fiber reinforced concrete", ACI 544.1R-96, American Concrete Institute.

[4] ACI Committee 544, 2006. State of the art report on fiber reinforced concrete, ACI 544,1R-82. American Concrete Institute, Detroit.

[5] ACI Committee 544, 2006. Design considerations for steel fiber reinforced concrete, ACI 544,4R-89. American Concrete Institute, Detroit.

[6] F. Altun et al. "Effects of steel fiber addition on mechanical properties of concrete and RC beams", Construction and building Materials. Pp. 655-661.

[7] Ashour S. A., Hasanian G. S. and Wafa, F. F. 1993. "Flexural Behavior of High Strength Fiber Reinforced Concrete Beams". ACI Structural Journal, V90, No. 3 May-June, pp279-287.

[8] Ashour S. A., Hasanian G. S. and Wafa, F. F. 1992. "Shear Behavior of High-Strength Fiber Reinforced Concrete Beams", ACI Structural Journal, March-April, V.89, No. 2, pp 176- 184.

[9] S. Yazici et al. "Effect of aspect ratio and volume fraction of steel fiber on the mechanical properties of SFRC", Construction and building material, pp. 1250-1253.

[10] K. Holschemacher et al, "Effect of steel fibers on mechanical properties of high strength concrete", Materials and designs, pp. 2604-2615.

[11] M. Musmar, 2013 "Tensile strength of steel fiber reinforced concrete", Contemporary Engineering Sciences, Vol. 6, no. 5, 225-237.

[12] Carreira D.J., Chu K.H., 1985. "Stress-strain relationship for plain concrete in compression", ACI Journal 182(6):797-804.

[13] Nataraja M.C., Dhang N. and Gupta A.P., 1999. Stress strain curves for steel-fiber reinforced concrete under Compression. Cement and Concrete Composites. 21: 383-390.

[14] ABAQUS 6.10. 2011. ABQUS User's Manual. Dassault Systemes Simulia Corp., Providence, RI, USA.

[15] H. Khederzadeh, 2014. "Development of innovative designs of bridge barrier system incorporating reinforcing steel or GFRP bars", Ph.D. Thesis, Ryerson University, Toronto, Ontario, Canada.